Neutral speciation in realistic populations

Erik D. Nelson

Address: Department of Biophysics, University of Texas Southwestern Medical Center, 6001 Forest Park Blvd., Room ND10.214, Dallas, Texas 75235–9050

E–mail: nelsonerikd@gmail.com

Abstract

de Aguiar et al. have shown that basic patterns of species diversity found in nature can be described by a simple neutral model of speciation in which species emerge as a consequence of local mating and mate preference for genetic similarity. Their results have been cited as support for the neutral theory of biodiversity. However, because the mutation rates considered in their work are much larger than those experienced by living organisms, there is still some question as to whether speciation will occur in the neutral model under realistic conditions. Here, I develop a variant of the neutral model that includes a realistic mechanism for organism dispersal. I explore speciation in the model for a class of mobile organisms (butterflies), and I find that speciation does occur under conditions consistent with butterfly populations, albeit on narrow landscapes. The model also appears to exhibit scaling behavior – specifically, if the model is "scaled up" by increasing the area of the landscape while holding its length to width ratio and population density constant, the number of species tends to an asymptotic value. The results suggest that it is possible to infer speciation patterns in large populations by simulating much smaller, computationally tractable populations.

Keywords: Topopatric speciation, neutral theory of biodiversity, scaling, Heliconius.

Introduction

A classical view of speciation is that reproductive barriers between species emerge as a consequence of genetic divergence. In other words, genetically different individuals in a population are less likely to mate, or when they do mate, are more likely to produce offspring of lower fitness. In this way, a population may progressively separate into sub–populations that are rarely able to form viable hybrids via interbreeding. This sort of reasoning has led to models of speciation in which mate preference, or offspring fitness explicitly depend on the genetic distance between mating partners (for an excellent review of these models see [1, 2]).

In recent work, de Aguiar et al. have investigated a series of speciation models based on this principle [3–11]. Their approach is a generalization of the random mating model developed by Higgs and Derrida [12, 13] to local mating in spatially distributed populations. In both versions of the model, genomes are described as sequences of binary genes; Mutations are neutral, and occur at a rate μ per gene per generation. Individuals α and β are permitted to mate only when $q^{\alpha\beta}$, a measure of genetic similarity, exceeds a threshold value, q_{min}. In the local mating version of the model, the potential mates of a focal individual are limited to a specific range of its position on a two dimensional landscape. Under certain conditions (e.g. on population density, mutation rate, etc.) de Aquiar et al. find that a genetically uniform population will, over time, spontaneously divide into reproductively isolated clusters of individuals – i.e., into species – a process they refer to as "topopatric" speciation. Their approach is remarkably successful in predicting the basic patterns of biodiversity found in nature [3, 9]. However, because the mutation rates considered in their work are much larger than those experienced by real organisms, it is still unclear whether topopatric speciation will occur under realistic conditions.

To explain this, it is necessary to be specific about what a gene in the model represents in an organism. A useful example for this purpose is Heliconius, an intensely studied genus of butterfly species [14, 15]. The most recent estimate for the mutation rate in Heliconius is 2.9×10^{-9} per nucleotide site per generation [16]. The effective population size corresponding to this estimate is $N = 2\times10^6$. The average length of a Heliconius gene can be estimated from Drosophila (an organism used to identify butterfly genes) as $\Delta L \simeq 1770$ nucleotides [17], which results in a mutation rate per gene of about $\mu = 5.1 \times 10^{-6}$ per generation. If we assume that a single nucleotide mutation in a Heliconius gene corresponds to a gene mutation in the neutral model, then the scaled mutation rate, $N\mu$, is already in range of the values $N\mu \overset{\sim}{>} 0.025$ that lead to speciation in [3]. In random mating models (specifically, in the Wright–Fisher model [18]), populations with the same value of $N\mu$ are known to exhibit similar steady state distributions [19]. Since $N\mu$ for Heliconius is in range of the values leading to speciation in the neutral model, it is tempting to think that similar speciation patterns will occur for realistic values of N and μ.

However, there are a number of problems with this analysis. First, there is no guarantee that the scaling principles [19] which hold for random mating models [20] will hold for populations with local mating on spatially extended landscapes. Assuming they do hold, the analysis does not account for empirical genetic differences between incipient butterfly species, which are typically on the order of 1 percent or more [14, 15] (see also [21]). As a result, butterfly species will have many more mutational differences per gene (on average) than the analysis above permits.

This problem can be addressed by reconsidering the definition a gene segment. Let $d^{\alpha\beta}$ denote the genetic (Hamming) distance between two genomes g^α and g^β, and, for simplicity, assume that distances between diploid genomes are measured by comparing

paternal chromosomes only (i.e., so that $d^{\alpha\beta}$ corresponds to the number of sites that differ between paternal chromosomes). The degree of similarity between g^{α} and g^{β} can then be defined as

$$q^{\alpha\beta} = 1 - d^{\alpha\beta}/\,n \tag{1}$$

where n is the number of genes in a model genome. As noted above, mating between organisms α and β can occur in the model only when $q^{\alpha\beta}$ is greater than some q_{min}. If, at the same time, we require the fractional distance, f, between incipient species to be at least 1 percent ($f = 0.01$), and we again assume that a gene mutation in the model corresponds to a single nucleotide mutation in a butterfly gene, we obtain the following correspondence condition between genes in the model and genes in an organism,

$$(1 - q_{min})\,n = f\,n\,\Delta L \tag{2}$$

where ΔL is the length (to be determined) of an organismal "gene". In other words, given that a single nucleotide mutation in an organismal gene corresponds to a gene mutation in the model, the threshold number of mutational differences between model species is equal to the minimal number of mutational differences between incipient butterfly species. Let d_{max} denote the value of $d^{\alpha\beta}$ in Eq. (1) for which $q^{\alpha\beta}$ satisfies $q^{\alpha\beta} = q_{min}$. The value of d_{max} used by de Aguiar et al. is approximately $d_{max} = 0.06n$, leading to a similarity threshold $q_{min} = 0.94$ and a gene length $\Delta L = 6$ nucleotides (here, d_{max} corresponds to the parameter G in ref. [3]). Using the data above for Heliconius, one obtains $\mu \simeq 1.7 \times 10^{-8}$ per gene per generation (about three orders of magnitude smaller than the minimal value of μ used by de Aguiar et al.) and $N\mu \simeq 0.035$. Thus, according to these rough calculations, $N\mu$ is consistent with values leading to speciation in [3].

It is worth noting that the parameter choices for f and d_{max} in Eq. (2) are somewhat

arbitrary. For example, according to the data in [14] a more accurate value of f for Heliconius species might be $f = 0.02$, which would result in a smaller value of ΔL, and thus a smaller value of μ; Larger values of d_{max} were also studied in [8] which will have the opposite effect on μ. In addition, while I have used the effective population size for Heliconius to estimate $N\mu$, it may be more accurate to consider the actual (census) population size, which is usually larger. Finally, population sizes and site mutation rates vary among organisms (mammals, fish, birds, etc. [22]). While it is of interest to explore all of these conditions, simulations of neutral speciation in such large populations are daunting, even on modern parallel computers (see below). In addition, data for population size and site mutation rate in many different organisms [22] lead to values of $N\mu$ that are similar in order of magnitude to the value estimated for Heliconius (given similar values of f and d_{max}). Thus, simulations under conditions for butterfly populations should shed some light on whether topopatric speciation occurs in general. Does topopatric speciation occur under these conditions?

In this work, I develop a straight forward version of the neutral model sketched above that incorporates the flight patterns of butterflies in order to address this question. Individuals in the model have diploid genomes, and evolve on a continuous landscape. Mating is sexual, and occurs in discrete generations. In each generation, each female in the population randomly selects a mating partner from among the male individuals within a radius R of its current position. The mean number of offspring produced by each female is determined so as to maintain the local density of individuals at a fixed mean value. Offspring then disperse from the mating site in random directions according to an exponential flight length distribution [23] to start the next generation.

I explore scaling of the model to realistic population sizes and mutation rates by increasing the area of the landscape at constant population density while holding $N\mu$

fixed at a value consistent with Heliconius. Due to the large population sizes considered here ($N > 10^5$), I employ a novel approach to define species clusters. Instead of solving the eigenvalue problem in [5] for the whole population, I sample a fraction of the population, and use a rapid clustering algorithm [24, 25] to partition the sampled genomes by genetic distance. The clustering algorithm iteratively divides a sample into increasing numbers of clusters, and I select the partitioning with the largest number of clusters subject to the condition that the fixation index, F, a widely used measure of distance between genome clusters, satisfies $F > F^\star$ for all pairs of clusters in the partitioning, where $F^\star \overset{\sim}{>} 0.25$, consistent with incipient species in natural populations [14,15] (later below, I demonstrate this condition leads to very reasonable results for within species and between species genetic distances). The general behavior of the model as a function of population density, population size, and time is qualitatively similar to the models studied by de Aguiar et al. However, I find that persistent species occur only on narrow landscapes (with length to width ratio $\overset{\sim}{>} 5$) as realistic values of N and μ are approached. In this limit, populations with the same density, on landscapes with the same length to width ratio "scale" with population size, as described above. Below, I describe the model in more detail, and then discuss the results of my simulations.

Model

The genetic component of the model is similar to that considered by Schneider et al. [8]. Model genomes consist of two binary chromosomes, each of length n genes. During mating, genomes undergo a model form of meiosis (Fig. 1). In male meiosis, each chromosome is duplicated, and crossovers occur at random between maternal and paternal copies at a rate of 1 crossover per meiosis resulting in a set of four model gametes [26]. The same procedure is conducted for female genomes but with no crossing over, consistent with

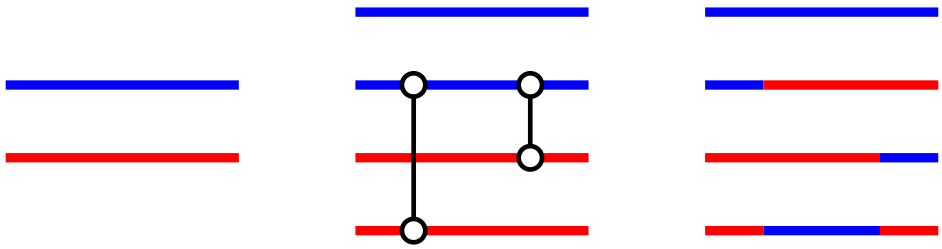

Fig. 1 Model meiosis. Chromosomes (left) are duplicated to produce a set of four model chromatids (middle). Random connections (vertical lines) occur between maternal (red) and paternal (blue) chromatids, and genetic material is exchanged to the right of the connection points (circles) producing a set of four model gametes (right).

butterfly reproduction. A gamete is selected at random from each set, and the selected gametes are combined to form a given offspring genome. The sex of an offspring is assigned at random. This process (including meiosis) is repeated a number of times for each mating event, depending on the number of offspring to be produced for a given female (see below).

Genetic distances between genomes are determined according to the "incomplete dominance" scheme used by Schneider et al. [8]: Let $g^{\alpha}_{\gamma,i} \in \{0,\, 1\}$ denote the state of gene i on chromosome $\gamma \in \{1, 2\}$ in genome α, and let $\phi^{\alpha}_{i} \in \{0, \frac{1}{2}, 1\}$ denote the average of $g^{\alpha}_{\gamma,i}$ over γ, $\phi^{\alpha}_{i} = \frac{1}{2}\sum_{\gamma} g^{\alpha}_{\gamma,i}$. Distances between genomes are defined as,

$$d^{\alpha\beta} \;=\; \sum_{i} \left|\phi^{\alpha}_{i} \;-\; \phi^{\beta}_{i}\right| \tag{3}$$

such that the effects of mutations at site i in chromosomes $\gamma \in \{1, 2\}$ are additive. The fixation index for a pair of genome clusters μ and $\nu \neq \mu$ is computed as [27]

$$F_{\mu\nu} \;= 1 \;-\; \frac{\delta_{\mu\nu}}{\Delta_{\mu\nu}} \tag{4}$$

where $\delta_{\mu\nu}$ denotes the average distance between genomes α and $\beta \neq \alpha$, both in cluster μ, or both in cluster ν, and $\Delta_{\mu\nu}$ denotes the average distance between genomes α in cluster

μ, and β in cluster ν. Accordingly, I refer to $\delta_{\mu\nu}$ and $\Delta_{\mu\nu}$ as the average within cluster and between cluster distances, respectively. Note that when genomes in clusters μ and ν are similar, $\delta_{\mu\nu} \simeq \Delta_{\mu\nu}$ so that $F_{\mu\nu} \simeq 0$.

The simulations proceed as follows: A population of N identical genomes is first spread across the landscape at random. Initially, genomes contain no mutations (i.e., $g^{\alpha}_{\gamma,i} = 0$ uniformly). In stage (i) of the algorithm, each individual undergoes a single random flight of mean length $\lambda = 1$, distributed as $f(x) = \lambda^{-1} \exp -x/\lambda$. The boundaries of the landscape are reflective (see Online resource 1). In stage (ii), each female randomly selects a mate from among males within a distance $R = \lambda$ of its position on the landscape, subject to the requirement that $q^{\alpha\beta} \geq q_{min}$ where $q_{min} = 0.95$. The number of offspring produced in a given mating event is Poisson distributed with mean

$$n^{\alpha}_{o} = \frac{A^{\alpha}/n^{\alpha}_{f}}{\sum_{\gamma} A^{\gamma}/n^{\gamma}_{f}} N \tag{5}$$

where A^{γ} is the area of overlap between the landscape and the mating circle for genome γ, n^{γ}_{f} is the total number of female genomes within the mating circle (including γ itself), and the sum over γ in Eq. (5) is restricted to mated female genomes (see Online resource 1). As a result, the average total number of offspring produced is equal to N, and the number of offspring produced in a particular mating event decreases with the local density of females, reflecting the availability of resources in a natural population. Finally, in stage (iii), offspring genomes undergo random mutations, and are deposited at the positions of their respective female parents. The parent generation is removed, and the procedure starts again from stage (i).

Each of the simulations below run for $4N$ generations, and are sampled at intervals of $\Delta t = 100$ generations. In all simulations, the mutation rate is $\mu = 0.05/N$ per gene

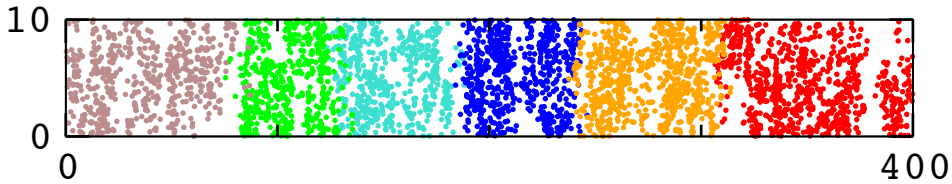

Fig. 2 Snapshot of the speciation pattern taken during the simulation in Fig. 3 described later below.

per generation, slightly larger than the estimate above based on the effective population size for Heliconius. Populations evolve on landscapes of width w and length l. The mean number of individuals is $N = l\,w\,\rho$, where ρ is the mean number of individuals per unit area; Here, I consider the values $\rho = 4$, 8, and 16, consistent with density and flight length data available for non–migratory butterflies (this data is discussed in detail later below). I focus on the case $\rho = 4$ for which the average number of individuals in a mating circle, $\pi R^2 \rho$, is consistent with typical values simulated by de Aguiar et al. in [5–8]. Here and below, species clusters (Fig. 2) are computed from random samples of size $\min\{N/4, 10^4\}$ individuals. To determine the number of species, I examine all partitionings up to 20 clusters. Genomes are partitioned using the "average" method defined in [25]. In all of the simulations, $F^\star = 0.24$. The unit of length in the model is arbitrary, however, since $\lambda = 1$, all length parameters are in effect expressed in units of λ. For the species considered here, a typical value for λ would be in the range $\lambda = 0.1 - 1$ km. The data in this work were generated using a multi–thread algorithm [28] which divides the computational overhead of the simulations among 32 processor cores. The timescale for individual simulations ranges from hours to weeks depending on N.

Results

To verify the model, I first examined some basic statistics along a trajectory. Fig.

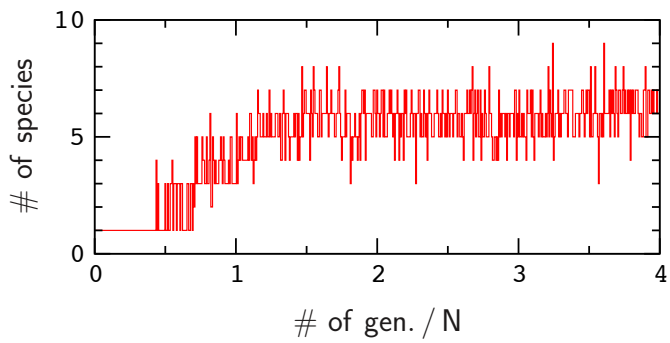

Fig. 3 Number of species, $\nu(t)$, for a simulation with $\rho = 4$, $n = 10^3$ and $F^\star = 0.24$. The dimensions of the landscape are the same as in Fig. 3. $\nu(t)$ increases for smaller values of $F^\star$.

3 shows the number of species, $\nu(t)$, as a function of time, t (where t is the number of generations) for a simulation with $\rho = 4$ and chromosome length $n = 10^3$. In general, $\nu(t)$ reaches a steady state after about N generations. Fig. 4 shows the relationship between $F_{\mu\nu}$, $\Delta_{\mu\nu}$ and $\delta_{\mu\nu}$ for partitionings sampled during the simulation in Fig. 3; A

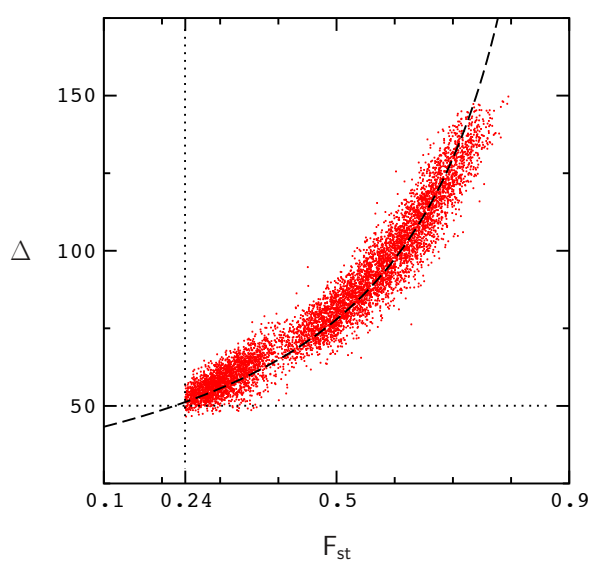

Fig. 4 Correlation between $\Delta_{\mu\nu}$ and $F_{\mu\nu}$ for partitions selected during the simulation in Fig. 3. The dashed line is a fit to the function $\Delta = \delta \,/\, (1 - F)$ leading to $\delta \simeq 39$. Dotted lines indicate the values of $F^\star$ and d_{max} used in the simulation.

fit of the function $\Delta = \delta \,/\, (1 - F)$ obtained from Eq. (4) to the data for $\Delta_{\mu\nu}$ versus $F_{\mu\nu}$ yields $\delta \simeq 39$ (correlation coefficient of 0.97). Notice that the smallest sampled distances between clusters have $\Delta_{\mu\nu} \sim 50$, in agreement with the value $d_{max} = 50$ used in the simulation (recall that $q_{min} = 0.05$).

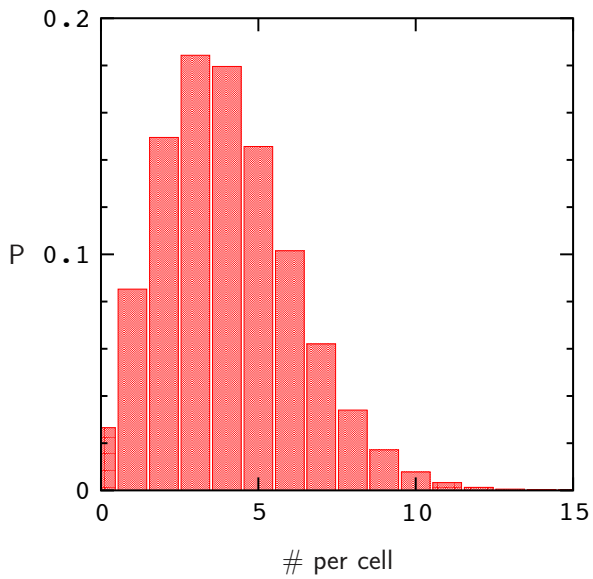

Fig. 5 Probability distribution for the number of individuals per grid cell (see text) for the simulation in Fig. 3.

In Fig. 5, I compute the local density of individuals during the simulation by overlaying the landscape with a square grid (with grid spacing λ) and then counting the number of individuals contained in each grid cell. Fig. 5 plots the probability distribution for the occupancy of grid cells (results for larger values of ρ are provided in Online resource 1). Fig. 6 shows the probability distribution for the number of mating events per male; The average number of mating events is 1, as expected for equal densities of male and female individuals.

The remaining figures describe speciation in the model as it is scaled toward realistic values of N and μ. As noted above, this is accomplished by increasing the area of the

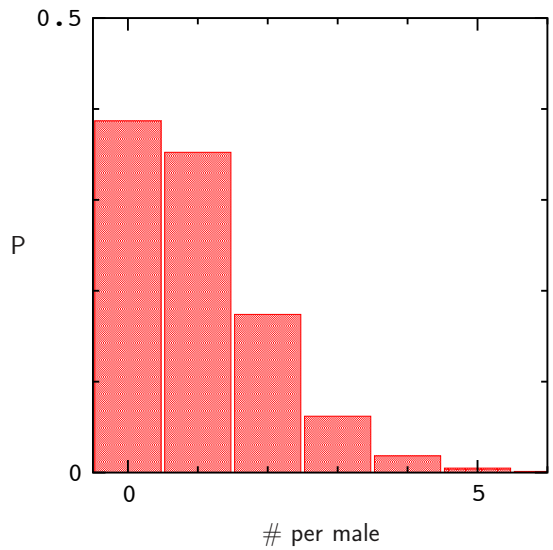

Fig. 6 Probability distribution for the number of mating events per male individual for the simulation in Fig. 3.

landscape at constant ρ with $N\mu = 0.05$. Fig. 7 describes the average number of species in the steady state region, $\langle \nu \rangle_{t>N}$, for $\rho = 4$ and landscapes with fixed width and increasing length. Each data point corresponds to a single simulation of length $4N$. In this case,

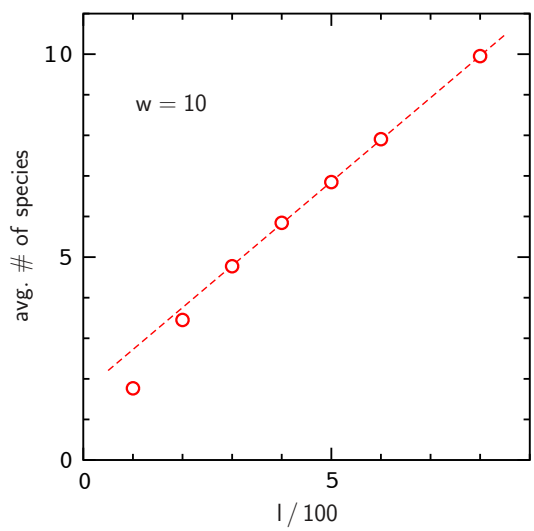

Fig. 7 Number of species, $\langle \nu \rangle_{t>N}$, versus landscape length for simulations with $\rho = 4$, $n = 10^3$, and $F^\star = 0.24$. The dashed line is a fit to the data for $l/100 > 2$.

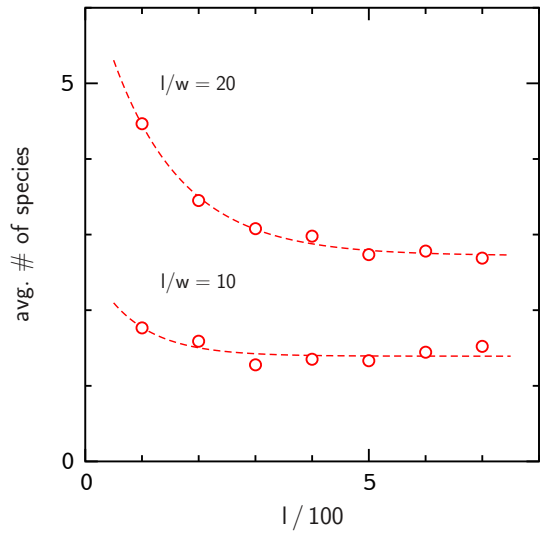

Fig. 8 Number of species, $\langle\nu\rangle_{t>N}$, versus landscape length for landscapes with fixed length to width ratio. The parameters are $\rho = 4$, $n = 10^3$, and $F^\star = 0.24$. Dashed lines are fits of the function $f(l) = \alpha + \beta\ \exp(-\gamma l)$ to the data.

$\langle\nu\rangle_{t>N}$ increases roughly linearly as the area of the landscape is increased, ultimately resulting in a narrow, almost 1–dimensional landscape as μ and N approach the values estimated for Heliconius "genes" via the condition $N\mu = 0.05$. By contrast, $\langle\nu\rangle_{t>N}$ levels off with increasing area if the length to width ratio of the landscape is held constant (Fig. 8). In this case, simulations with relatively small population sizes roughly predict the behavior of $\langle\nu\rangle_{t>N}$ in much larger populations. Thus, the scaling rule described appears to hold asymptotically for a given population density and length to width ratio. An additional plot for $l/w = 100/7$ is provided in Online resource 1. The time scales of the simulations for the larger populations in these figures prevented an investigation of larger population densities.

The results in Fig. 8 suggest that speciation will occur for $l/w \stackrel{\sim}{>} 10$. However, the data in [4] suggest that $\langle\nu\rangle_{t>N}$ is sensitive to genome length. To explore this possibility, I computed $\langle\nu\rangle_{t>N}$ for increasing genome lengths on fixed landscapes (Fig. 9). Increasing

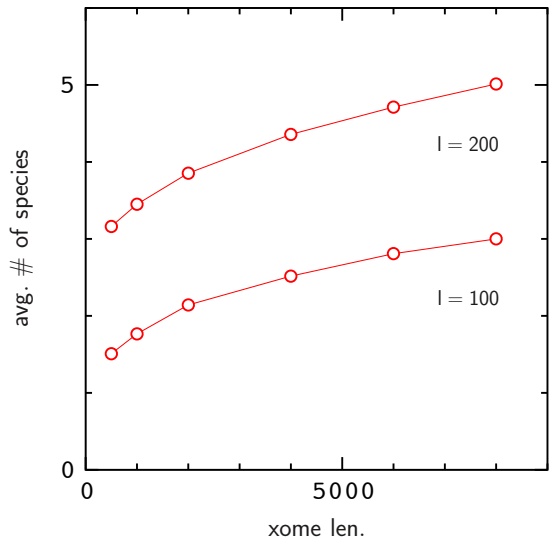

Fig. 9 Number of species, $\langle \nu \rangle_{t>N}$, versus chromosome length for landscapes with fixed dimensions. In both plots, $w = 10$ and $\rho = 4$.

the length of the genomes clearly seems to enhance speciation, however, I find that this effect decreases significantly with increasing population density (see Online resource 1).

I also examined the dependence of $\langle \nu \rangle_{t>N}$ on population density. Fig. 10 describes the effect of increasing density on $\langle \nu \rangle_{t>N}$ for landscapes with fixed width $w = 10$ and increasing length (as in Fig. 7). For each landscape length, $\langle \nu \rangle_{t>N}$ decreases with increasing density. This result is consistent with the effect of increasing the mating radius (and, consequently, the number of individuals in the mating circle) in ref. [8]. The effect of increasing the landscape width at higher densities is shown in Online resource 1.

Discussion

The results clearly show that persistent species will appear in the model if it is continued to population sizes and mutation rates typical of butterflies; However, this depends on the dimensions of the landscape, and seems limited to those with length to width ratio

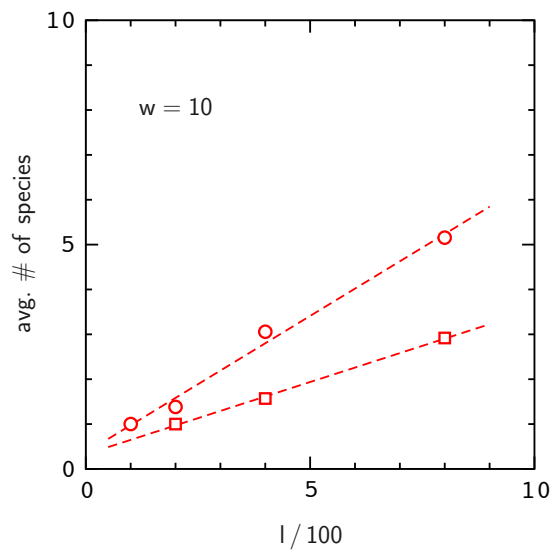

Fig. 10 Number of species, $\langle \nu \rangle_{t>N}$, as in Fig. 7 for higher population densities, $\rho = 8$ (circles), and $\rho = 16$ (squares).

$\tilde{>}$ 10, or perhaps $\tilde{>}$ 5 depending on genome length, $F^\star$, and other parameters used in the simulations. The dependence of $\langle \nu \rangle_{t>N}$ on the length to width (aspect) ratio of the landscape is consistent with the results in [3] where, for a given landscape area, species are much more abundant on 1–dimensional landscapes (i.e., with $l/w \gg 1$) than fully 2–dimensional landscapes with $l/w = 1$. A possible explanation for this effect is that persistent clusters are easier to maintain on narrow landscapes since they are exposed to gene flow from other species on only two small fronts (Fig. 2), whereas for $l/w = 1$ species clusters tend to be fully exposed [3,4]. In addition, the dispersal mechanism used here leads to more rapid gene flow across the landscape than the mechanism used by de Aguiar et al. Thus, given the small value of $N\mu$ used here, it is not difficult to see why speciation might be limited to narrow landscapes in the present model.

Aside from the parameters f and d_{max} already discussed, the results depend on the limit $F^\star$, and the population size used in the estimate for $N\mu$. Smaller values of $F^\star$ will obviously lead to larger values of $\langle \nu \rangle_{t>N}$. In this work, I have used a conservative value

for $F^\star$, however, a smaller value, such as $F^\star = 0.2$, might also be considered reasonable, and would lead to a noticeable increase in $\langle \nu \rangle_{t>N}$ (but also to noisier trajectories for $\nu(t)$). It is also important to remark that natural resource distributions are often confined to narrow, or coastal regions, and are usually textured or fragmented in ways that can promote speciation [29, 30].

As noted earlier, the relationship between flight length and population density was constructed to agree with the parameters available for butterflies. While population density estimates are available for many types of butterfly, flight length data seems limited to threatened species; I was able to find both parameters for two species – the Fender's blue and the Glanville fritillary. For Fender's blue, Schultz and Crone estimate the average length of a single flight within a resource patch at 2.1 m, with about 2100 such flights per lifetime [23]. Assuming a random walk, this leads to a per generation flight length of about $\lambda = 0.1$ km. From the data available in [23], the typical number of individuals within an area of size λ^2 is between 3–5. For the Glanville fritillary [31], I obtain a rough estimate for the per generation flight length of about $\lambda = 1$ km, and a population density of between 2–12 individuals per km^2 [32]. The density values used in the simulations (in particular, the value $\rho = 4$) are consistent with these estimates.

Finally, while the data in Fig. 8 clearly indicate scaling behavior, more data is needed to confirm this result over a wider range of population sizes and densities. Unfortunately, despite parallelization of the problem, a study of this kind would be very difficult with the present algorithm (for example, the largest populations in Fig. 8 ($N \simeq 2.5 \times 10^5$) required over three weeks of simulation time – a requirement that grows linearly with population size). More realistic population sizes of order 10^6 or larger should be tractable on graphical processing units, where the number of available processor cores is orders of magnitude larger [33]. This sort of approach could provide a much clearer picture of

neutral speciation in natural populations.

Acknowedgments: I thank Nick Grishin for providing access to computer facilities during part of this work.

References

[1] Gavrilets S (2014) Models of speciation: Where are we now? *J. Hered.* 105:743–755.

[2] Kopp M (2010) Speciation and the neutral theory of biodiversity. *BioEssays* 32:564–570.

[3] de Aguiar MAM, M. Baranger M, Baptestini EM, Kaufman L, Bar-Yam Y (2009) Global patterns of speciation and diversity. *Nature* 460:384–387.

[4] de Aguiar MAM (2017) Speciation in the derrida–higgs model with finite genomes and spatial populations. *J. Phys. A* 50:085602.

[5] de Aguiar MAM, Bar-Yam Y (2011) Moran model as a dynamical process on networks and its implications for neutral speciation. *Phys. Rev. E* 84:031901.

[6] Baptestini EM, de Aguiar M (2013) The role of sex separation in neutral speciation. *Theor. Ecol.* 6:213–223.

[7] Baptestini EM, de Aguiar M, Bar-Yam Y (2013) Conditions for neutral speciation via isolation by distance. *J. Theor. Biol.* 335:51–56.

[8] Schneider D, Baptestini EM, de Aguiar M (2016) Diploid versus haploid models of neutral speciation. *J. Biol. Phys.* 42:235–245.

[9] Martins AY, de Aguiar M, Bar-Yam Y (2013) Evolution and stability of ring species. *J. Theor. Biol.* 335:51–56.

[10] Costa CLN, et al. (2019) Signatures of microevolutionary processes in phylogenetic patterns. *Syst. Biol.* 68:131–144.

[11] Caetano RA, Sanchez S, Costa CLN, de Aguiar MAM (2020) Sympatric speciation based on pure assortative mating. *J. Phys. A* 53:155601.

[12] Higgs PG, Derrida B (1991) Stochastic models for species formation in evolving populations. *J. Phys. A* 24:L985–L991.

[13] Higgs PG, Derrida B (1992) Genetic distance and species formation in evolving populations. *J. Mol. Evol.* 35:454–465.

[14] Kronforst MR, et al. (2013) Hybridization reveals the evolving genomic architecture of speciation. *Cell Rep.* 5:666–677.

[15] Van Belleghem SM, et al. (2018) Patterns of z chromosome divergence among heliconius species highlight the importance of historical demography. *Mol. Ecol.* 27:3852–3872.

[16] Keightley PD, et al. (2014) Estimation of the spontaneous mutation rate in heliconius melpomene. *Mol. Biol. Evol.* 32:239–243.

[17] Wilke CO (2004) Molecular clock in neutral protein evolution. *BMC Genetics* 5:25.

[18] Gillespie JH (2004) *Population genetics, a concise guide.* (Johns Hopkins University Press, Baltimore, MD).

[19] Felsenstein J (2016) Theoretical evolutionary genetics (https://felsenst.github.io/pgbook/pgbook.html). see p. 350.

[20] Nelson ED, Grishin NV (2019) How often do protein genes navigate valleys of low fitness? *Genes* 10:283–293.

[21] Cong Q, Zhang J, Grishin N (2019) Genomic determinants of speciation in butterflies (https://www.biorxiv.org/content/10.1101/837666v1).

[22] Bergeron LA, et al. (2023) Evolution of the germline mutation rate across vertebrates. *Nature* 615:285–291.

[23] Schultz CB, Crone EE (2001) Edge mediated dispersal behavior in a prairie butterfly. *Ecology* 82:1879–1892.

[24] Dalitz C (2021) C++ fast hierarchical clustering algorithms (https://github.com/cdalitz/hclust-cpp).

[25] Mulliner D (2013) fastcluster: Fast hierarchical, agglomerative clustering routines for r and python. *J. Stat. Soft.* 53:1–9.

[26] Veller C, Kleckner N, Nowak MA (2018) A rigorous measure of genome–wide genetic shuffling that takes into account crossover positions and mendel's second law. *Proc. Natl. Acad. Sci. USA* 116:1659–1668.

[27] Bhatia G, Patterson N, Sankararaman S, Price AL (2013) Estimating and interpreting fst: The impact of rare variants. *Gen. Res.* 23:1514–1521.

[28] Mattson TG, He YH, Koniges AE (2019) *The OpenMP common core.* (MIT Press, Cambridge, MA).

[29] M'Gonigle LK, Mazzucco R, Otto SP, Dieckmann U (2012) Sexual selection enables long-term coexistence despite ecological equivalence. *Nature* 484:506–509.

[30] Princepe D, et al. (2022) Diversity patterns and speciation processes in a two-island system with continuous migration. *Evolution* 76:2260–2271.

[31] Fountain T, et al. (2018) Inferring dispersal across a fragmented landscape using reconstructed families in the glanville fritillary butterfly. *Evol. Appl.* 11:287–297.

[32] Hanski I, Meyke E (2005) Large scale dynamics of the glanville fritillary buterfly: Landscape structure, population processes, and weather. *Ann. Zool. Fennici.* 42:379–395.

[33] Ansorge R (2022) *Programming in parallel with CUDA*. (Cambridge University Press, Cambridge, UK).